DOI: 10.21062/mft.2023.062 http://www.journalmt.com

Analysis of Cutting Forces with Application of the Discrete Wavelet Transform in Titanium Ti6Al4V Turning

Paweł Karolczak (0000-0002-0595-1580)
Wrocław University of Science and Technology, Faculty of Mechanical Engineering, wyb. Wyspiańskiego 27, 50-370 Wroclaw, Poland, E-mail: pawel.karolczak@pwr.edu.pl

The paper presents the possibilities of using the wavelet transform to filter the cutting force signal. Tests were carried out by dry turning on the Ti6Al4V alloy with variable cutting parameters. Four blades with different nose geometry and coatings were used. From the recorded waveforms, the mean values of the force component F_c and the load stability coefficient *kn* were calculated. The measured force waveforms were filtered with Daubechies 4 (db4) and Daubechies 6 (db6) wavelets. From the ratio of the load stability after filtration to the load stability before filtration, the noise and disturbance values generated during the turning of the tested alloy and the force measurement were estimated. The research conducted shows how the machining conditions affect the forces and stability values, and thus also the variability of the cutting edge load when turning a titanium alloy. They also show the effectiveness of the Discrete Wavelet Transform (DWT) in separating the noise from the force signal.

Keywords: Titanium alloys, Cutting forces, Wavelet analysis, Load stability, Measurement distrurbances

1 Introduction

Due to their properties, such as high specific strength, the possibility of use in a high-temperature and corrosive environment, and good compatibility with human tissue, titanium alloys are widely used in many industries. They are used for the production of means of transport elements, mainly aeroplanes and helicopters [1,2]. In addition, they are used to produce machine components in the food and chemical industries. An important application is implanted knee and hip joints [2,3,4]. New titanium alloys with better biocompatibility and lower toxicity are being developed [5]. The high requirements for items made of titanium alloys have it turned out that the dominant method of their processing should be machining. However, the low thermal conductivity, high hardness and strength, low value of the longitudinal elasticity modulus, high tendency to work hardening, and high chemical reactivity of titanium alloys make them difficult to machine materials [6]. Taking into account the properties of titanium alloys already presented, it should be stated that planning their machining is difficult and must be carried out with high accuracy. When titanium alloys are machining, high temperatures are created in the machining zone, affecting faster cutting blade wear [7] and makes the surface layer thicker and the changes more severe [8]. Moreover, the aforementioned high hardness and tensile strength are associated with high cutting forces and, as a result, with the deformation of the cutting tools [9]. The problem of blade wear can be minimised by using machining methods such as electrical discharge machining EDM for both titanium alloys [10] and nickel alloys [11]. Unfortunately, the so-called white layer, i.e. the heat-affected zone (HAZ), which is often present in the workpiece, means that this type of manufacturing technique cannot fully replace machining. To improve the machinability of titanium alloys and lower the cutting temperature, the process is assisted by cutting fluids. The use of flood cooling, compared to dry machining, allows a significant improvement in surface quality, a reduction in total blade wear of 30%, a reduction in diffusion and adhesive tool wear, as well as a much lower adhesion of chips to the blade rake face and, as a result, increased production efficiency [12]. Even better results are obtained when the coolant is applied under high pressure. The contact length of the chip with the tool is then reduced and they are broken more effectively. The tool life is increased by 75% compared to machining with flood cooling. Unfortunately, no positive change in the value of the cutting forces is observed [6]. Compared to dry machining, forces can be reduced by using oil mist aid [13, 14], especially when nanoparticles of various compounds, for example MoS_2, are added to the mist [15]. Furthermore, the use of oil mist significantly improves the surface quality of the titanium alloys machined [16].

Cutting forces are not such an important indicator of machinability as surface roughness or tool wear. However, the ability to predict and control them can significantly improve the surface quality and tool life of the blades. In turning, the cutting force is divided into 3 components: F_c is the main cutting force in the direction of the cutting speed, F_p is the back force in the direction of the turning tool, and F_f is the feed force in the direction of the feed. Since the components are dependent on each other and there is a correlation between them, most often only the F_c component is analysed. In abbreviated analyses, the average value of the main cutting force is usually used. However, to obtain information on the nature of the force and its possible impact on the process, the maximum and minimum values, and thus the amplitude of the force, must not be ignored. The machining process is very often unstable, therefore, large fluctuations in force values may occur. This fact additionally disqualifies the average value from detailed analyses. Such fluctuations can be reduced in titanium machining by using cryogenic cooling in the process [17]. Force values are measured in experimental studies. They can also be predicted using appropriate models e.g. using deep neural network and regression analysis [18]. Predictive models work well for plastic metals, such as aluminium [19], as well as hard materials, such as titanium alloys [20, 21].

Cutting forces, like other signals received and measured in the process (vibrations, acoustic emission, surface roughness), belong to non-stationary values. Constant time and frequency resolutions in the Fourier transform are not suitable for the analysis of such signals. The solution to this problem is the use of the wavelet transform (WT). WT provides good resolution in both the time and frequency domains and can extract information in the time domain in different frequency bands [22, 23, 24]. In the past ten years, WT has become one of the most critical signal processing tools to monitor, eg, the condition of cutting tools [25] or to detect surface quality [26]. For example, Lee et al. [27] used both the FFT and the continuous wavelet transform (CWT) to detect the appearance of wear of ceramic inserts in the profile of the workpiece. Also, Dutta et al. [28] predicted tool wear values using the discrete wavelet transform (DWT) based on workpiece images. Ahmed et al. used the wavelet transform to separate the built-up edge (BUE) signals from the tool wear signals for real-time monitoring of the BUE height when turning AISI 304 stainless steel [29]. To separate the signals of blade wear and chip breaking, Tangjitsitcharoen et al. [30] used DWT. These signals differ significantly in frequency, and it is possible to separate them. On the other hand, the surface roughness values were determined by Pour in [31] using the hybrid algorithm based on the analysis of time series and DWT. Zając et al. used the wavelet transform to analyse the parameters of the Abbot-Firestone curve at subsequent decomposition levels [32]. The wavelet transform can be used to monitor and supervise the machining process of complex and heterogeneous materials. Li et al. [33] investigated the monitoring of the cutting force during the machining of carbon fibre reinforced polymer composites (CFRP) using discrete wavelet analysis with Daubechies wavelet (db3). Sudden detail factor peaks were correlated with fibre detachment (at high fibre angles). Plaza et al. [34] implemented real-time surface quality monitoring during CNC CFRP turning. Pahuja et al. used the transformation of wavelet packets to monitor edge milling [35]. The coefficients of the final wavelet packets at each decomposition level were used to calculate the spectrum of packet characteristics - arithmetic mean, standard deviation, energy, entropy, and energy entropy coefficient. In other works by Pahuja et al. [36] implemented continuous wavelet analysis in order to find the influence of fibre orientation on technological effects. They also used the transformation of wavelet packets to monitor the abrasive waterjet treatment of CFRP-Tytan stacks using acoustic emission signals [37]. The wavelet transform can be helpful in identifying interference and noise in the force signal. Cabrera et al. [38] used the discrete wavelet transform to decompose the force signal recorded during milling. This signal has been decomposed into an approximation and a detailed signal to minimise measurement noise. Moreover, in this work, the authors proved that the force signal, and especially its peak density, can be used to identify vibrations in the machining process. Tangjitsitcharoen et al. [39] used wavelet transform and Daubechies wavelets to distribute the measured feed force in turning. Moreover, in order to eliminate the effects of cutting conditions in force measurements, they determined the so-called force ratio, i.e. comparisons of amplitude to the value of static force. Karolczak [40] used a similar methodology to determine the noise of force measurements in the turning of aluminium composites.

The aim of the work was to determine the possibility of using DWT to effectively filter the cutting force during the turning of a difficult-to-machine titanium alloy. In addition, analysis of the average value of the main component of the cutting force does not give a complete picture of the load on the cutting edge. Therefore, the article uses the load constancy factor, which is the inverse of the load variation coefficient. The use of this factor in addition to the average force value is very important because it provides additional information about the cutting forces, especially the amplitude.

2 Test Conditions

A titanium alloy Ti6Al4V was tested. The chemical composition and selected properties of the alloy are shown in Tables 1 and 2. The turning tests were carried out on a TUR 560MN CNC universal lathe. Four cutting tools were used for the tests. First, they differed in the geometry of the blade. The two inserts had a traditional geometry with a nose rounding radius r_ε of 0.4 mm. Two more inserts had a special smoothing geometry called Wiper. This modification consists in the introduction of auxiliary smoothing edges with a very large rounding radius R_{b0} and, in some cases, auxiliary rounding edges $r_{\varepsilon 1}$ and $r_{\varepsilon 2}$ (Fig. 1). The inserts also differed in anti-wear coatings. Those marked 1025 were PVD coated and the coating consisted mainly of TiN. The coating on the 2015 marked blades was applied using the CVD method and its main component was (Ti,Al)N. Turning tests were carried out under changing cutting conditions. The main variable parameter was the feed *f*. Five feeds were used - 0.08; 0.13; 0.17; 0.21; 0.24 mm.rev^{-1}. The tests were carried out at two cutting speeds v_c, 30 and 60 m.min^{-1}. The cut depth, a_p, was constant at 0.5 mm. The test conditions are summarised in Table 3.

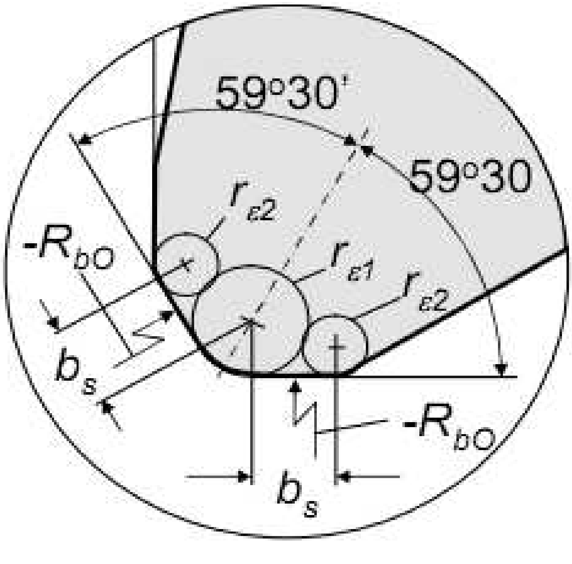

***Fig. 1** Wiper blade geometry [41]*

***Tab. 1** Chemical composition of tested material*

Elemental concentration [%]						
C	V	Al	O	N	Fe	Ti
0.03	4.04	6.46	0.16	0.01	0.05	rest

***Tab. 2** Selected properties of tested titanium alloy*

Strength properties			
Tensile strength Rm [MPa]	*Yield strength 0.2 Rp0.2 [MPa]*	*Elongation A [%]*	*Area reduction Z [%]*
980	*908*	*13*	*38*

***Tab. 3** Research conditions*

Machined Material	*Ti6Al4V*
Machine Tool	*CNC TUR 560MN*
Cutting Inserts	*TCMT 16 03 04 1025 MF – TiN coating, normal geometry* *TCMX 16 03 04 1025 WF – TiN coating, Wiper geometry* *TCMT 11 03 04 2015 MF – (Ti,Al)N coating, normal geometry* *TCMX 11 03 04 2015 WF – (Ti,Al)N coating, Wiper geometry*
Tool Holders	*STGCR 2020K 16* *STGCR 1616H 11*
Cutting Speed (m.min^{-1})	*30; 60*
Feed Rate (mm.rev^{-1})	*0.08; 0.13; 0.17; 0.21; 0.24*
Depth of Cut (mm)	*0.5*

The cutting forces that occur during the turning of the selected titanium alloy were analysed according to the methodology presented in Figure 2.

The first step in the analysis of the forces was to measure them. Cutting forces were measured using the measuring path (Fig. 3), which included the Kistler 9257A piezoelectric dynamometer, electric signal amplifier type 5011 and Tektronix Digital Phosphor Oscilloscope TDS 5054B.

Further analysis was limited to the main cutting force F_c. On the basis of the recorded waveforms, the mean values of the F_c component were first determined. For the calculation of the mean cutting force values, signal fragments with a constant number of points were selected. Assuming that the force changed its value during machining from F_{cmin} to F_{cmax}, these maximum and minimum force values were determined in the next step and then the amplitude F_{ca} for the main cutting force was calculated. The first stage of the force analysis was completed with the calculation of the load stability coefficient according to formula 1. This coefficient, which is the ratio of the mean value to the amplitude, shows how dynamic the force changes are and to what extent the force changes can impact the tool [41].

$$kn = {}^{F_c}/_{F_{ca}} \tag{1}$$

Since the measurement of cutting forces is disturbed by noise, which can introduce errors in the estimation of the force values, in the next stage of the analysis, it was decided to filter the measurements.

The purpose of the filtration was to remove noise caused by the operation of the machine engine, vibrations of the machine tool, or the environment. Filtration was carried out in Matlab using the wavelet analysis toolbox. It was decided to use wavelet analysis due to its numerous advantages. In this analysis, as in the Fourier analysis, the analysed signal is divided into waves. However, unlike Fourier's analysis. where the tested signal is divided into sine waves of different frequencies; in wavelet analysis the signal is divided into shifted and scaled versions of the original wavelet. When the sine wave diagram and the example wavelets are compared, it can be seen that the signals with sharp changes (and such a signal is the cutting force) can be more precisely analysed with just such an irregular wavelet. Wavelet analysis enables the discovery of certain properties of the tested signal that may be ignored by other signal analysis techniques, e.g. discontinuities of higher derivatives or the similarity of signal fragments. In addition, wavelet analysis also allows compression and denoising of the signal without significant degradation. To remove signal noise, a discrete wavelet transform (DWT) is used, in which the raw signal is filtered twice, through a high-pass filter (wavelet) and a low-pass filter (scaling function assigned to the wavelet). Two sequences are obtained, one is called approximation, it is a noise-cancelled signal of force, and the other is a detail that is a noise. It is possible to successively filter the obtained approximation on successive decomposition levels until a completely noise-free signal is obtained.

A very crucial point in analysis is the selection of the wavelet. The shape of the wavelet should be as close to the shape of the analysed signal as possible. Two wavelets from the Daubechies family were selected for the analysis of cutting forces in the turning of the Ti6Al4V alloy. These wavelets belong to the family of orthogonal wavelets with a compact carrier. It is the compactness of their support and the fairly uncomplicated form that are their biggest advantages. The Daubechies 4 (less compact) and Daubechies 6 (more compact) wavelets were selected for analysis. The choice of two wavelets was dictated by a different nature (compactness) of the course of forces during high-feed and low-feed machining. After the wavelets were selected in the Matlab programme, fragments of the cutting force waveforms were analysed. Noise-free waveforms and noises were obtained. Next, similarly as in the case of raw measurements, the mean values, the amplitudes and the load stability factors were calculated. Finally, the ratio of the coefficient of load stability of the force filtered by each wavelet to the load stability of the force calculated from the raw measurement was calculated. An increase in the load stability means that the disturbances were filtered out and removed by particular wavelets. Therefore, the degree of increase of the *kn* coefficient may indicate the amount of noise and disturbance.

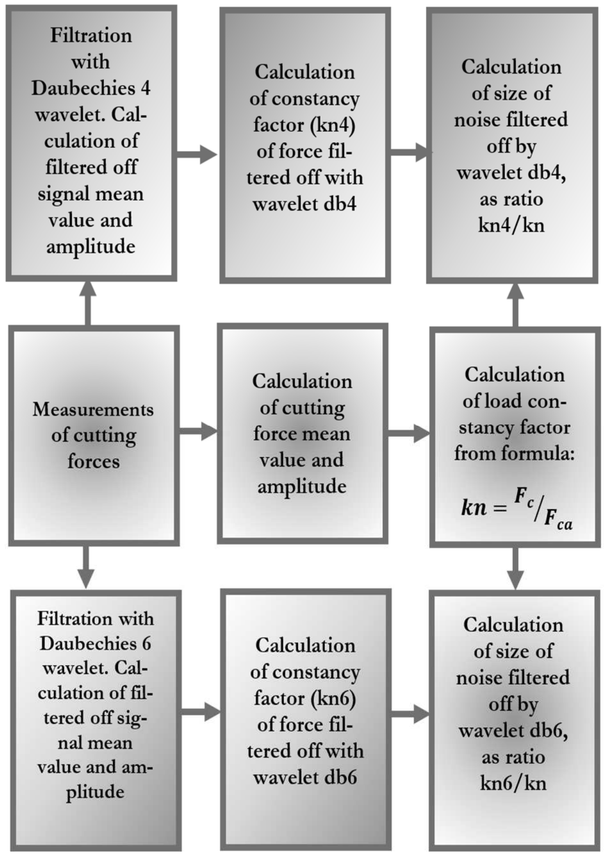

***Fig. 2** Cutting force analysis algorithm*

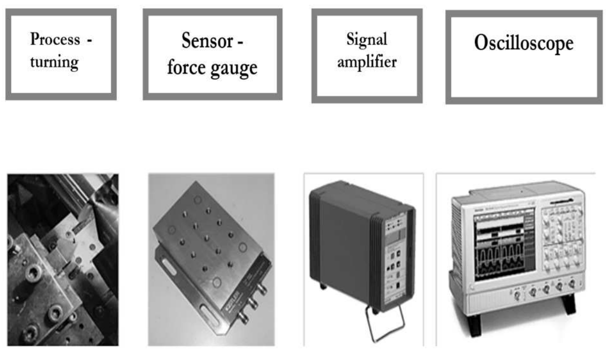

***Fig. 3** Cutting forces measurement path*

3 Test Results and Discussion

3.1 Cutting force measurements results

Tables 4-7 show the mean values of the measured F_c component, the load stability factor calculated from the measurements, the values of this factor after filtering with the wavelet transform, and the noise values determined.

Tab. 4 *Results of measurements and analyzes of cutting forces generated during turning of Ti6Al4V alloy with an insert TCMT 16 03 04 1025 MF*

v_c/f (m.min^{-1})/ (mm.rev^{-1})	Mean F_c (N)	kn	kn after db4 filtration	noise after db4 filtration	kn after db6 filtration	noise after db6 filtration
30/0.08	195.15	3.03	5.44	1.80	5.56	1.84
30/0.13	225.37	2.91	4.32	1.48	4.44	1.52
30/0.17	238.99	2.78	3.88	1.40	3.91	1.41
30/0.21	257.57	2.40	2.90	1.21	2.91	1.21
30/0.24	284.13	2.28	2.67	1.17	2.69	1.82
60/0.08	214.38	4.98	10.21	2.05	10.56	2.12
60/0.13	228.56	5.31	9.60	1.81	9.81	1.86
60/0.17	232.95	4.92	8.26	1.68	8.14	1.65
60/0.21	251.09	4.49	7.39	1.65	7.59	1.69
60/0.24	284.72	4.41	7.19	1.63	7.32	1.66

Tab. 5 *Results of measurements and analyzes of cutting forces generated during turning of Ti6Al4V alloy with an insert TCMX 16 03 04 1025 WF*

v_c/f (m.min^{-1})/ (mm.rev^{-1})	Mean F_c (N)	kn	kn after db4 filtration	noise after db4 filtration	kn after db6 filtration	noise after db6 filtration
30/0.08	173.29	2.81	5.93	2.11	6.23	2.21
30/0.13	186.73	3.10	6.46	2.08	6.89	2.22
30/0.17	195.55	3.50	7.14	2.04	7.49	2.14
30/0.21	210.65	4.08	7.95	1.95	8.60	2.11
30/0.24	218.81	4.24	8.38	1.98	9.00	2.12
60/0.08	186.56	4.34	6.74	1.55	7.55	1.74
60/0.13	192.21	4.47	7.57	1.69	7.72	1.73
60/0.17	196.49	4.57	8.54	1.87	9.36	2.05
60/0.21	203.14	4.72	9.36	1.98	9.77	2.07
60/0.24	208.46	4.85	9.48	1.96	10.37	2.14

Tab. 6 *Results of measurements and analyzes of cutting forces generated during turning of Ti6Al4V alloy with an insert TCMX 16 03 042015 MF*

v_c/f (m.min^{-1})/ (mm.rev^{-1})	Mean F_c (N)	kn	kn after db4 filtration	noise after db4 filtration	kn after db6 filtration	noise after db6 filtration
30/0.08	204.02	2.97	4.68	1.58	4.98	1.68
30/0.13	241.26	3.12	4.72	1.52	5.01	1.61
30/0.17	242.22	2.82	4.93	1.75	5.12	1.82
30/0.21	262.28	3.21	6.02	1.87	6.61	2.06
30/0.24	276.05	3.78	6.12	1.62	6.77	1.79
60/0.08	214.90	4.16	6.05	1.45	6.07	1.46
60/0.13	226.45	4.39	7.35	1.68	7.50	1.71
60/0.17	244.40	4.74	8.23	1.74	8.43	1.78
60/0.21	262.95	5.10	8.51	1.67	9.19	1.81
60/0.24	280.24	4.65	9.28	1.99	9.73	2.09

Tab. 7 *Results of measurements and analyzes of cutting forces generated during turning of Ti6Al4V alloy with an insert TCMX 16 03 04 2015 WF*

v_c/f (m.min-1)/ (mm.rev-1)	Mean F_c (N)	kn	kn after db4 filtration	noise after db4 filtration	kn after db6 filtration	noise after db6 filtration
30/0.08	195.83	2.68	4.09	1.53	4.70	1.75
30/0.13	224.36	3.26	4.37	1.34	4.94	1.52
30/0.17	229.35	3.33	4.46	1.34	5.03	1.51
30/0.21	230.83	2.98	4.49	1.51	5.13	1.72
30/0.24	232.67	3.86	5.40	1.40	5.97	1.54
60/0.08	193.17	2.99	4.72	1.57	4.84	1.62
60/0.13	209.06	4.05	6.41	1.58	6.81	1.68
60/0.17	219.25	4.25	6.64	1.56	7.07	1.66
60/0.21	228.74	4.09	6.67	1.63	7.33	1.79
60/0.24	238.86	5.05	7.40	1.47	7.58	1.50

By analysing the data contained in the tables, we can conclude that higher average values of the F_c component were generated during machining with traditional geometry tools. This applies to both tested coatings, but with the TiN coating the difference is greater and reaches even 36%. According to theory, the force values increase with increasing feed. The highest measured value of force F_c for an insert with a TiN coating was 284.72 N, and for an insert with a (Ti, Al)N coating 280.24 N. The lowest values were measured during turning with a feed of 0.08 mm.rev-1 and amounted to 173.29 N and 195.83, respectively. The influence of cutting speed is insignificant (Figs. 4 and 5).

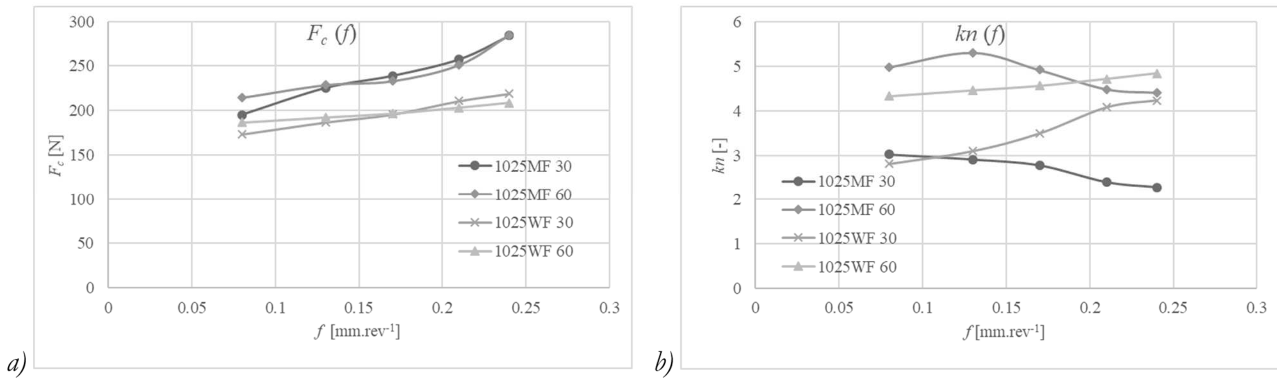

Fig. 4 *F_c cutting force (a) and load stability coefficient kn (b) as a function of feed during turning with a TiN-coated blade*

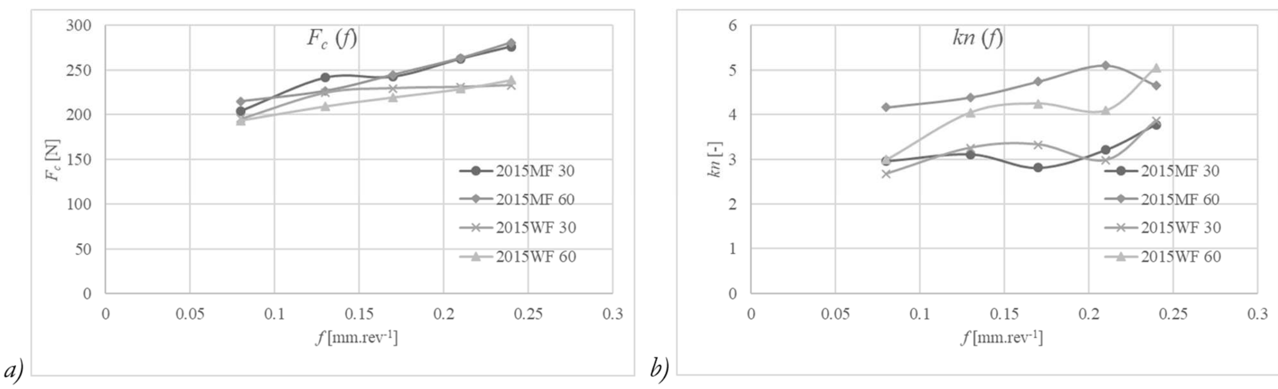

Fig. 5 *F_c cutting force (a) and load stability coefficient kn (b) as a function of feed during turning with a (Ti,Al)N-coated blade*

The values of the load stability coefficient calculated from the measured signal during turning with a TiN coated blade as a function of feed are shown in Figure 4. Its changes are different from the mean force values. The only relationship that can be noticed is that this coefficient increases with the higher cutting speed. The influence of the feed is unclear. For blades with a smoothing geometry, it increases with the higher feed. In turning with a conventional geometry blade, it decreases with higher feed or increases slightly with the lowest feed. The highest value of the *kn* factor for 1025 inserts is 5.31, the smallest is 2.28.

The values of the load stability coefficient calculated from the measured force signal during turning with a coated blade (Ti,Al)N in the feed function are shown in Figure 5. It has higher values when turning with a higher cutting speed. It can also be seen that, for both geometries, in principle, this factor increases with the higher feed. However, this is not a linear or square increase. This relationship can be described by a polynomial of the third or fourth degree. However, it can also be assumed that sudden changes in the *kn* coefficient may be dictated by disturbances in the cutting process that superimposed on the force signal and strengthened it. Such an assumption makes it justifiable to filter the measurement in order to separate the force waveform from disturbances and noise.

3.2 Analysis of research results

Examples of Daubechies 4 and Daubechies 6 wavelet filtration are shown in Figure 6. The figure shows the forces that occur when turning the Ti6Al4V alloy with a TCMT16 03 04 1025 MF insert with a cutting speed of v_c=30 m.min^{-1}, f =0.17mm.rev^{-1}. The first waveforms from the top (red - s) represent the measured cutting force. The blue waveforms a1 are waved-filtered cutting force signals. Waveforms d1 - d3 (green) are the noise recorded and filtered out by wavelets, at successive filtration levels, which constitute measurement disturbances. When comparing the images shown in Figure 6, one can see slightly higher noise values, obtained during filtration with the db6 wavelet.

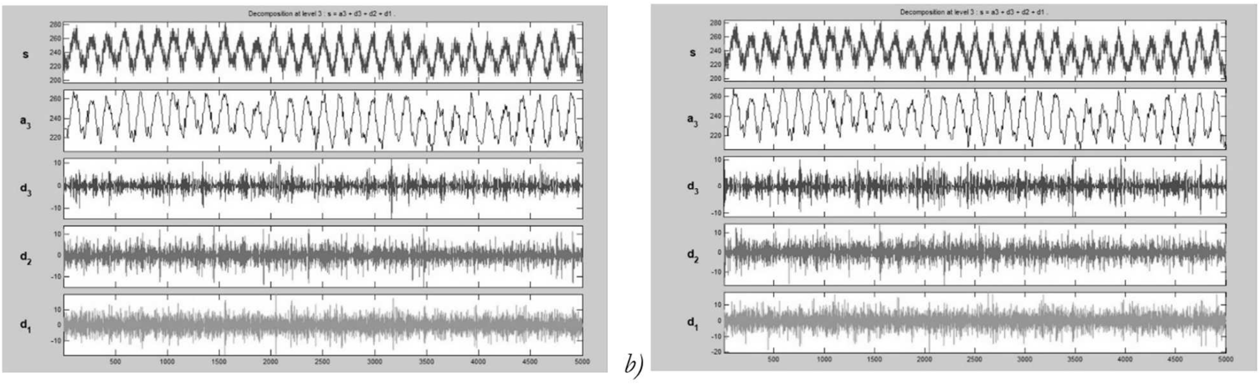

Fig. 6 *Discrete wavelet transform in Matlab. Daubechies 4 (db4) wavelet filtration (a). Daubechies 6 (db6) wavelet filtration (b)*

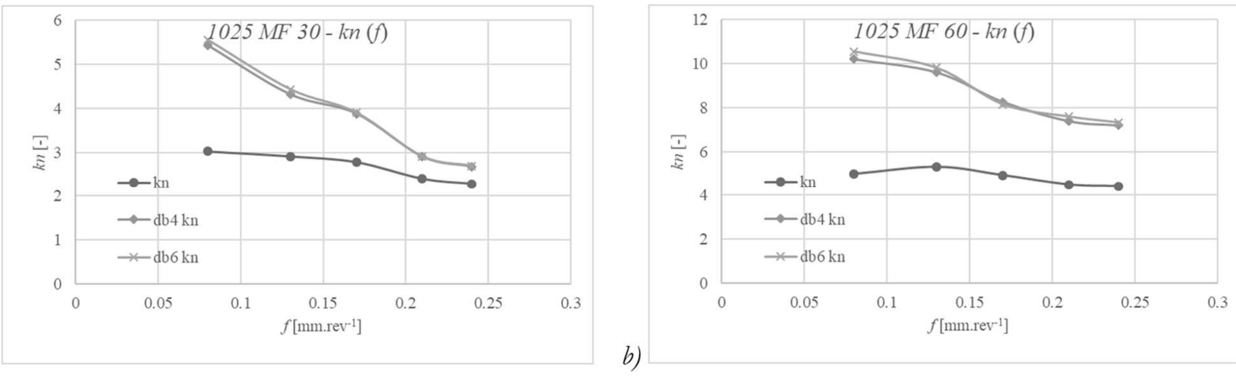

Fig. 7 *Kn coefficient calculated from the measurements and after db4 and db6 wavelet filtration as a function of the feed rate for turning with a TCMT 16 03 04 1025 MF insert, a) turning with v_c = 30m.min^{-1}, b) turning with v_c = 60m.min^{-1}*

Fig. 7 shows the graphs of the load stability coefficient as a function of the feed before and after wavelet filtration, calculated for the forces occurring during machining with the TCMT160304 1025MF insert. The load stability determined for the unfiltered signal decreases slightly with increasing feed. With a cutting speed of v_c = 30m.min^{-1} and a feed rate of 0.08, the value is 3.03, and for a feed rate of 0.24, it is already 2.28. Higher values of load stability were found during turning at a cutting speed of 60 m.min^{-1}. This coefficient varies in the range of 4.41-5.31. After separating by wavelets the force signal from the measurement disturbances, the load stability factor increases significantly. For turning at 30 m.min^{-1} and db4 wavelet filtration, the increase is 78% at a feed of 0.08 and 17% at a feed of 0.24 mm.rev^{-1}. A greater increase was recorded for the higher speed, 83% and 18%, respectively. In the case of machining with the TCMT 160304 1025MF tool, the difference in the filtration power with the db4 and db6 wavelets is not noticeable. Furthermore, after the disturbances have been removed, a clear decrease in the stability of the load is visible with an increase in the feed, especially at a lower cutting speed. For the feed of 0.08 it is twice as large as for the feed of 0.24 mm.rev^{-1}.

Figure 8 shows the graphs of the load stability, before and after filtration, for turning with the TCMX160304 1025WF blade. Changing the geometry of the insert from traditional to smoothing makes the dependence of the coefficient on the feed changes. *Kn* increases with increasing of this cutting parameter. It is especially visible at a speed of 30 m.min^{-1}; the increase is 50%. For twice the cutting speed, it is only 12%. After filtering out the noise, the increase in *kn* with increasing feed for both speeds is similar and amounts to about 40%. In addition, the load stability during turning with a Wiper blade is higher by up to 93% than when machining with a traditional blade and reaches a value of even 5.31. It is worth noting that the influence of the type of wavelet selected is already visible. The more compact wavelet (db6) treats the greater amount of the measurement signal as a disturbance. After filtration with this wavelet, the *kn* coefficient increased by 110-122%, and with the db 4 wavelet by 94-110%.

Figure 9 shows the coefficients of load stability determined from the force F_c generated during turning with a blade with traditional geometry and coated (Ti, Al) N. The *kn* values calculated from the measurement are within the range of 2.97 -3.78 for a cutting speed of 30m / min and between 4.16 and 5.1 for double the speed. The influence of the feed is ambiguous. On the other hand, the positive effect of the increase in cutting speed is clear. Again, a slightly greater increase in load stability can be observed after filtration with the db6 wavelet compared to the db4 wavelet. Regardless of the cutting speed, the greatest increase in *kn* after filtration was recorded for the feed 0.21 mm.rev^{-1}, respectively 87% for the Daubechies 4 wavelet and 105% for the Daubechies 6 wavelet. When comparing the blades with traditional geometry, it can be stated that higher load stability and therefore less variability occur for a tool with a TiN coating only for the speed of 60 m.min^{-1} and feeds in the range of 0.08-0.17 mm.rev^{-1} and for the speed of 30 m.min^{-1} and the feed 0.08. For the most productive cutting parameters, higher load stability occurs during turning with a coated (Ti, Al)N insert.

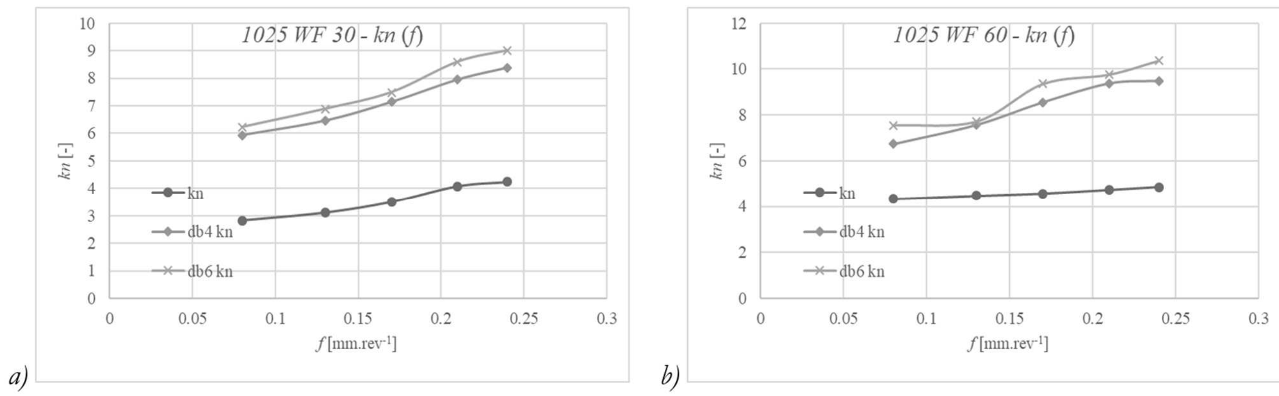

Fig. 8 *Kn coefficient calculated from the measurements and after db4 and db6 wavelet filtration as a function of the feed rate for turning with a TCMX 16 03 04 1025 WF insert, a) turning with v_c = 30m.min^{-1}, b) turning with v_c = 60m.min^{-1}*

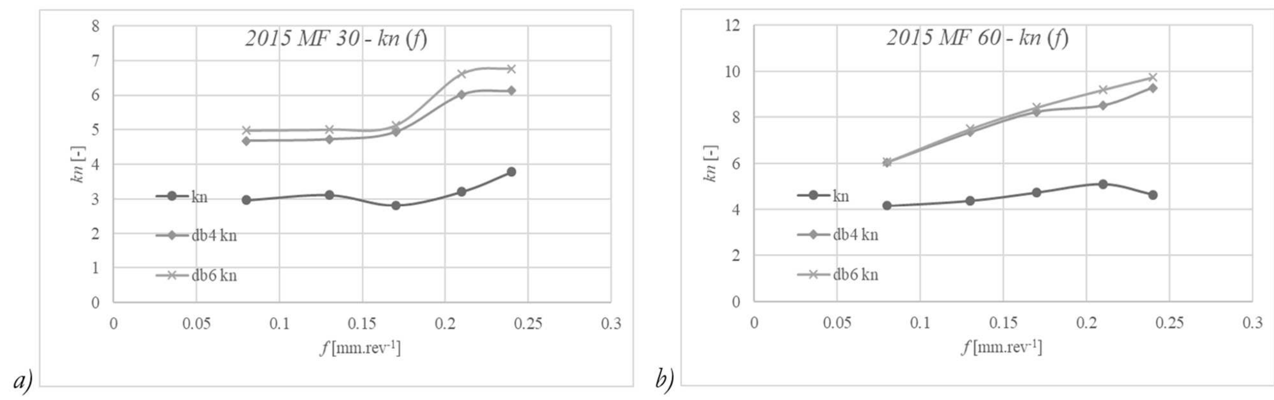

Fig. 9 *Kn coefficient calculated from the measurements and after db4 and db6 wavelet filtration as a function of the feed rate for turning with a TCMT 16 03 04 2015 MF insert, a) turning with v_c = 30m.min^{-1}, b) turning with v_c = 60m.min^{-1}*

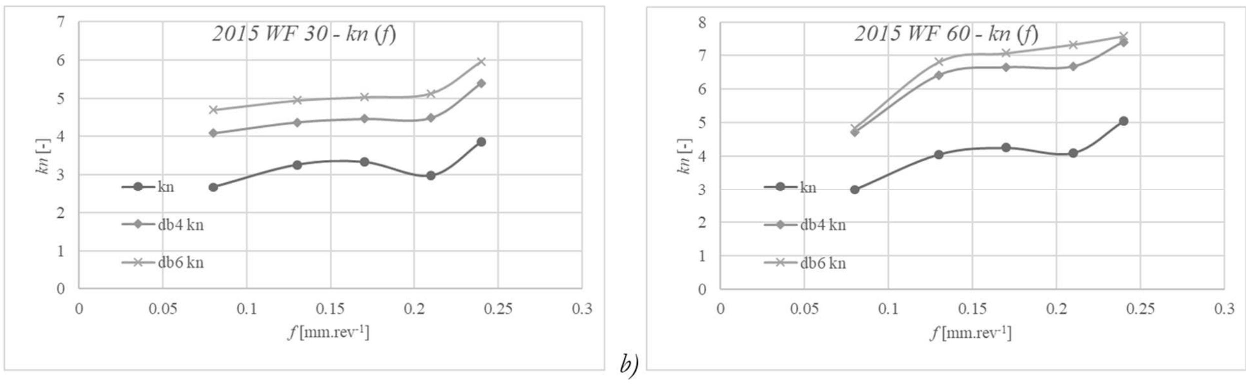

Fig. 10 *Kn coefficient calculated from the measurements and after db4 and db6 wavelet filtration as a function of the feed rate for turning with a TCMX 16 03 04 2015 WF insert, a) turning with v_c = 30m.min^{-1}, b) turning with v_c = 60m.min^{-1}*

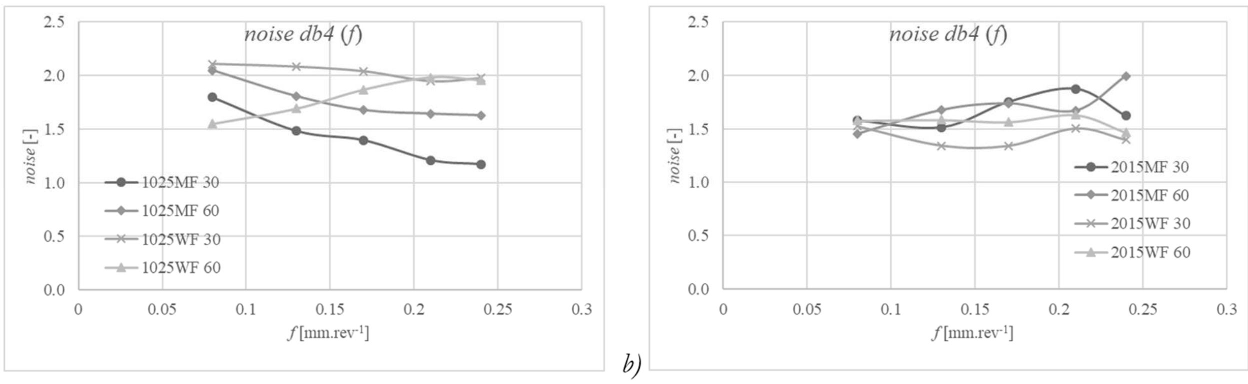

Fig. 11 *Noise and disturbance values calculated with the db 4 wavelet, in turning with TiN coated blades (a) and (Ti, Al)N (b)*

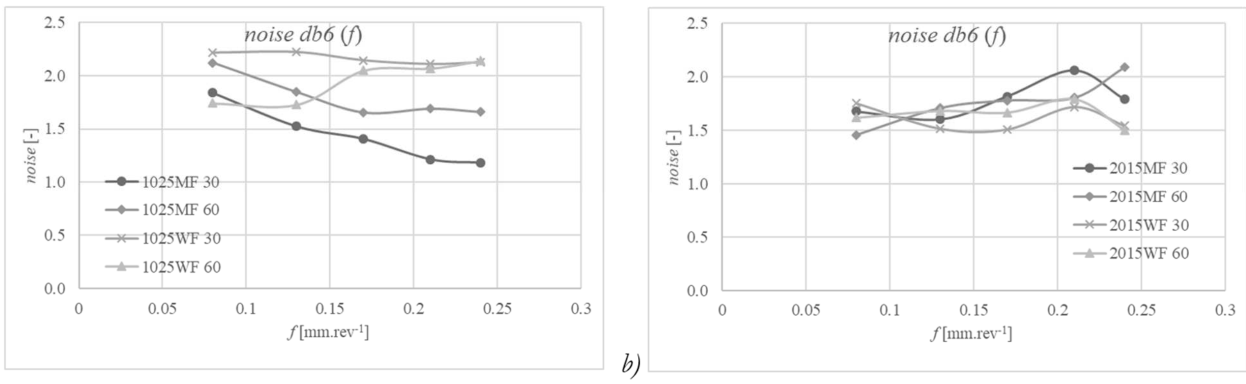

Fig. 12 *Noise and disturbance values calculated with the db 6 wavelet, in turning with TiN coated blades (a) and (Ti, Al)N (b)*

Figure 10 shows the values of the load stability factor as a function of the feed for the forces measured during turning with a smoothing and coated (Ti, Al)N blade. As with other tools, the *kn* factor becomes larger when machined at higher cutting speeds. It is influenced by lower average force values, which in turn may result from lower adhesion at the tool-chip-workpiece interface. *Kn* increases to a feed of 0.17, then decreases slightly to increase again for a feed of 0.24. The smoothing geometry in the blade makes the *kn* generally smaller than for blades with traditional geometry. After separating the force from the disturbances, *kn* increases by 34-63% for the db4 wavelet and by 50-79% for the db6 wavelet. The difference in the filtration strength between the wavelets is the greatest for machining with these blades.

Figures 11 and 12 show the noise values calculated by DWT that occur during the measurement of cutting forces in turning of the Ti6Al4V alloy. Turning with a TiN coated blade, noise decreases with increasing feed. Only for the smoothing blade and the speeds of 60m.min^{-1}, they increase with the higher cutting speed. This case makes it impossible to draw general conclusions about the effect of geometry or cutting speed. For a tool with a second coating, the dependence of noise on cutting parameters or geometry is even more ambiguous. This result may be a confirmation of the assumption that the discrete wavelet transform effectively separates the force signal from the disturbance. The size of the disturbance in the cutting process may, of course, change functionally as the machining conditions change. Furthermore, the level of disturbances is influenced by random quantities such as heterogeneity and defects of the machined material, chip flow, tool wear process, thermal changes on the machine tool, its vibrations, and the environment in the production hall.

4 Conclusions

The titanium alloy Ti6Al4V was tested. Turning tests were carried out with blades with traditional or smoothing geometry and coated with PVD or CVD coatings. The cutting forces were measured, and then the obtained waveforms were subjected to discrete wavelet transform. When the load stability calculated from the filtered and raw waveforms was compared, the disturbances that occurred during the turning process were estimated. On the basis of the results of the research, it was found that:

- the size of force measurement disturbances does not depend directly on the process parameters; the value of disturbances, and thus the measurement of force, is largely influenced by random factors,
- the discrete wavelet transformation allows us to separate the force signal from disturbances, a after filtering the dependence of the load stability on the treatment conditions is more regular,
- the filtration with the use of a more compact wavelet is stronger compared to filtration with a less compact wavelet; the cutting parameters do not affect this effect,
- the load stability increases with the higher feed, only for a tool with a traditional geometry coated with TiN, this relationship is not maintained,
- further research is needed on the possibility of using DWT to filter the cutting force signal.

References

[1] ABBAS AT, SHARMA N, ANWAR S, LUQMAN M, TOMAZ I, HEGAB H. Multi-response optimization in high-speed machining of Ti-6Al-4V using TOPSIS-fuzzy integrated approach. *Materials*. 2020;13(5): 1104. https://doi.org/10.3390/ma13051104

[2] MIERZEJEWSKA Ż, KUPTEL P, SIDUN J. Analysis of the surface condition of removed bone implants. Eksploatacja i Niezawodnosc - *Maintenance and Reliability*. 2016;18(1): 65–72. http://dx.doi.org/10.17531/ein.2016.1.9

[3] HREN I, KUŚMIERCZAK S, HORKÝ R, MACH J. Analysis of the Effect of Heat Treatment and Corrosion Load on the Microstructure and Microhardness of the Ti6Al4V Alloy. *Manufacturing Technology*. 2022;22(4):414-422. doi: 10.21062/mft.2022.058.

[4] ROUDNICKA M, BAYER F, MICHALCOVA A, KUBASEK J, GHASSAN E, ALZUBI H, VOJTECH D. Biomedical titanium alloy prepared by additive manufacturing: Effect of processing on tribology. *Manufacturing Technology* 2020, 20(6):809-816 | DOI: 10.21062/mft.2020.112

[5] VONAVKOVA I, VOJTECH D, PALOUSEK D. Characterization of β-Ti alloy prepared by SLM method. *Manufacturing Technology*. 2020;20(5):690-696. doi: 10.21062/mft.2020.091

[6] PIMENOV DP, MIA M, GUPTA MK, MACHADO AR, TOMAZ IV, SARIKAYA M, WOJCIECHOWSKI S, MIKOŁAJCZYK T, KAPŁONEK W. Improvement of machinability of Ti and its alloys using cooling lubrication techniques: a review and future prospect. *Journal of Materials Research and Technology*. 2021:11: 719-753 https://doi.org/10.1016/j.jmrt.2021.01.031 .

[7] GRZESIK W, NIESŁONY P, HABRAT W. Investigation of the tribological performance of AlTiN coated cutting tools in the machining of Ti6Al4V titanium alloy in terms of demanded tool life. Eksploatacja i Niezawodnosc - *Maintenance and Reliability*. 2019:21(1): 153–158. http://dx.doi.org/10.17531/ein.2019.1.17

[8] EZUGWU E, BONNEY J, YAMANE Y. An overview of the machinability of aeroengine alloys. *Journal of Materials Processing Technology*. 2003:134(2): 233-53. https://doi.org/10.1016/S0924-0136(02)01042-7.

[9] HABRAT W. *Analiza i modelowanie toczenia wykończeniowego tytanu i jego stopów*. Oficyna Wydawnicza Politechniki Rzeszowskiej. 2019. Rzeszów

[10] BHUI AS, SINGH G, SIDHU SS, BAINS PS. Experimental investigation of optimal ED machining parameters for Ti-6Al-4V

biomaterial. *Facta Universitatis Series: Mechanical Engineering*. 2018:16(3): 337-345. https://doi.org/10.22190/FUME180824033B

[11] SINGH A, GHADAI RK, KALITA K, CHATTERJEE P, PAMUČAR D. EDM process parameter optimization for efficient machining of Inconel – 718. *Facta Universitatis Series: Mechanical Engineering*. 2020:18(3): 473-490 https://doi.org/10.22190/FUME200406035S

[12] MUTHUKRISHNAN N, DAVIM PJ. Influence of coolant in machinability of titanium alloy (Ti-6Al-4V). *Journal of Surface Engineered Materials and Advanced Technology*. 2011;1(1): 9-14. https://doi.org10.4236/jsemat.2011.11002.

[13] DEIAB I, RAZA SW, PERVAIZ S. Analysis of lubrication strategies for sustainable machining during turning of titanium Ti-6Al-4V alloy. *Procedia CIRP*. 2014;17: 766–771.

[14] GRGURAS D, STERLE L, PUSAVEC F. Cutting forces and chip morphology in LCO2 + MQL assisted robotic drilling of Ti6Al4V. *Procedia CIRP*. 2021;102: 299–302

[15] GAURAV G, SHARMA A, DANGAYACH GS, MEENA ML. Assessment of jojoba as a pure and nano-fluid base oil in minimum quantity lubrication (MQL) hard-turning of Ti6Al4V: A step towards sustainable machining. *Journal of Cleaner Production*. 2020;272; 122553 https://doi.org/10.1016/j.jclepro.2020.122553

[16] NI C, WANG X, ZHU L, LIU D, WANG Y, ZHENG Z, ZHANG P. Machining performance and wear mechanism of PVD TiAlN/AlCrN coated carbide tool in precision machining of selective laser melted Ti6Al4V alloys under dry and MQL conditions. *Journal of Manufacturing Processes*. 2022;79: 975–989

[17] LIU H, AYED Y, BIREMBAUX H, ROSSI F, POULACHON G. Impacts of flank wear and cooling strategies on evolutions of built-up edges, diffusion wear and cutting forces in Ti6Al4V machining. *Tribology International*. 2022;171: 107537

[18] GUO S, ZHENG H, LIU X, GU L. Comparison on Milling Force Model Prediction of New Cold Saw Blade Milling Cutter Based on Deep Neural Network and Regression Analysis. *Manufacturing Technology*. 2021;21(4):456-463. doi: 10.21062/mft.2021.053

[19] TSAI MY, CHANG SY, HUNG JP, WANG CC. Investigation of milling cutting forces and cutting coefficient for aluminum 6060-T6. *Computers and Electrical Engineering*. 2016;51: 320–330.

[20] ZHAO Z, TO S, ZHU Z, YIN T. A theoretical and experimental investigation of cutting forces and spring back behaviour of Ti6Al4V alloy in ultraprecision machining of microgrooves. *International Journal of Mechanical Sciences*. 2020;169: 105315

[21] YAMEOGO D, HADDAG B, MAKICH H, NOUARI M. Prediction of the cutting forces and chip morphology when machining the Ti6Al4V alloy using a microstructural coupled model. *Procedia CIRP*. 2017;58: 335 – 340.

[22] ZHU KP, WONG YS, HONG GS. Wavelet analysis of sensor signals for tool condition monitoring: a review and some new results. *International Journal of Machine Tools and Manufacture*. 2009;49(7-8): 537-553.

[23] FENG Z, LIANG M, CHU F. Recent advances in time–frequency analysis methods for machinery fault diagnosis: A review with application examples. *Mechanical Systems and Signal Processing*. 2013;38(1): 165-205.

[24] KRUEGER E, SCHEEREN EM, PACHECO RINALDIN CD, LAZZARETTI AE, NEVES EB, NOGUEIRA-NETO GN, NOHAMA P. Impact of skinfold thickness on wavelet-based mechanomyographic signal. *Facta Universitatis Series: Mechanical Engineering*. 2018;16(3): 359-368 https://doi.org/10.22190/FUME170602001K

[25] SHANBHAG VV, ROLFE BF, ARUNACHALAM N, PEREIRA MP. Investigating galling wear behaviour in sheet metal stamping using acoustic emissions. *Wear*. 2018;414–415: 31–42, https://doi.org/10.1016/j.wear.2018.07.003.

[26] GARCÍA PLAZA E, NÚÑEZ LÓPEZ PJ. Analysis of cutting force signals by wavelet packet transform for surface roughness monitoring in CNC turning. *Mechanical Systems and Signal Processing*. 2018;98: 634–651, https://doi.org/10.1016/j.ymssp.2017.05.006.

[27] LEE WK, RATNAM MM, AHMAD ZA. Detection of chipping in ceramic cutting inserts from workpiece profile during turning using fast Fourier transform (FFT) and continuous wavelet transform (CWT). *Precision Engineering*. 2017;47: 406–423

[28] DUTTA S, PAL SK, SEN R. Progressive tool flank wear monitoring by applying discrete wavelet transform on turned surface images. *Measurement*. 2016;77: 388–401, https://doi.org/10.1016/j.measurement.2015.09.028.

[29] AHMED YS, ARIF AFM, VELDHUIS SC. Application of the wavelet transform to acoustic emission signals for built-up edge monitoring in stainless steel machining. *Measurement*. 2020;154: 1074-1078 https://doi.org/10.1016/j.measurement.2020.107478

[30] TANGJITSITCHAROEN S, LOHASIRIWAT H. Intelligent monitoring and prediction of tool wear in CNC turning by utilizing wavelet transform. *International Journal of Advanced Manufacturing Technologies*. 2018;99(9): 2219–2230, https://doi.org/10.1007/s00170-017-1424-5.

[31] POUR M. Determining surface roughness of machining process types using a hybrid algorithm based on time series analysis and wavelet transform. *International Journal of Advanced Manufacturing Technologies*. 2018;97(9): 2603–2619, https://doi.org/10.1007/s00170-18-2070-2.

[32] ZAJAC J, MAKIEŁA W, STĘPIEŃ K, GOGOLEWSKI D. An Evaluation of Changeability of Parameters Describing Abbot Curve during a Wavelet Decomposition Process. *Manufacturing Technology*. 2014;14(4):665-671. doi: 10.21062/ujep/x.2014/a/1213-2489/MT/14/4/665.

[33] LI H, QIN X, HUANG T, LIU X, SUN D, JIN Y. Machining quality and cutting force signal analysis in UD-CFRP milling under different fiber orientation. *International Journal of Advanced Manufacturing Technologies*. 2018;98(9): 2377-2387. doi:10.1007/s00170-018-2312-3.

[34] GARCÍA PLAZA E, NÚŃEZ LÓPEZ PJ. Analysis of cutting force signals by wavelet packet transform for surface roughness monitoring in CNC turning. *Mechanical Systems and Signal Processing*. 2018;98: 634-651 doi:10.1016/j.ymssp.2017.05.006.

[35] PAHUJA R, MAMIDALA R. Quality monitoring in milling of unidirectional CFRP through wavelet packet transform of force signal. *Procedia Manufacturing*. 2020;48: 388–399

[36] PAHUJA R, MAMIDALA R. Process monitoring in milling unidirectional composite laminates through wavelet analysis of force signals. *Procedia Manufacturing*. 2018;26: 645-655 doi:10.1016/j.promfg.2018.07.075.

[37] PAHUJA R, MAMIDALA R. Surface quality monitoring in abrasive water jet machining of Ti6Al4V–CFRP stacks through wavelet packet analysis of acoustic emission signals. *International Journal of Advanced Manufacturing Technologies*. 2019;104: 4091-4104. doi:10.1007/s00170-019-04177-0.

[38] CABRERA CG, ARAUJO AC, CASTELLO DA. On the wavelet analysis of cutting forces for chatter identification in milling. *Advances in Manufacturing*. 2017;5(2): 130–142. DOI 10.1007/s40436-017-0179-4

[39] TANGJITSITCHAROEN S, LOHASIRIWAT H. Hybrid monitoring of chip formation and straightness in CNC turning by utilizing daubechies wavelet transform. *Procedia Manufacturing*. 2018;25: 279–286

[40] KAROLCZAK P. Application of Discrete Wavelet Transform to analysis of cutting forces in turning of Composites based on aluminium alloys reinforced with Al2O3 fibres. *FME Transactions*. 2021;49: 563-574. https://doi.org/10.5937/fme2103563K

[41] CICHOSZ P. *Narzędzia skrawające*. 2006: WNT Warszawa